Inorganica Chimica Acta, 48 (1981) 97–103

Spectroscopic Analysis of Mixed Valence Molybdenum Oxides

F. CARIATI

Istituto di Chimica Generale, Università di Sassari, Via Vienna 2, Sassari, Italy

J. C. J. BART

Montedison 'G. Donegani' Research Laboratories, Via G. Fauser 4, Novara, Italy

and A. SGAMELLOTTI

Dipartimento di Chimica, Università di Perugia, Via Elce di Sotto 10, Perugia, Italy

Received July 8, 1980

The cation valence state distribution in the higher molybdenum oxides $Mo_{18}O_{52}$, Mo_5O_{14}, $Mo_{17}O_{47}$ and Mo_4O_{11} has been studied by means of XPS spectroscopy in combination with bond-length:bond-strength relationships. Tetrahedral oxomolybdenum positions are occupied by Mo(VI), but considerable Mo(V)–Mo(VI) mixing is found in the other polyhedra (octahedra and pentagonal bipyramids), as also suggested by the observed Mo(3d) binding energies. Assignments of skeletal modes for these class II mixed valence systems are suggested.

Introduction

Although the stereogeometries of a variety of mixed valence compounds in the $MoO_{2.75}$–MoO_3 range are now fairly well established, their electronic structures require further elucidation. So far the interpretation of variations in the distortion of the oxomolybdenum polyhedra in terms of the nature and distribution of the cation states has been hampered by lack of detailed Mo–O bond-strength (s) bond-length (d) equations. As these have recently been worked out [1] a renewed attempt can be made to combine structural (XRD) and photoelectronic (XPS) data. Out of the seven mixed valence compounds within the composition range mentioned above [2], we have examined representatives of the three basic structure types (MoO_3, ReO_3 and mixed polygonal networks), namely $Mo_{18}O_{52}$, $Mo_{17}O_{47}$, Mo_5O_{14} and Mo_4O_{11} (Table I). Using criteria applied previously [3], we have also assigned to ν(Mo–O) infrared stretching vibrations.

Experimental

Materials

$Mo_{18}O_{52}$, $(Nb_{0.10}Mo_{0.90})_5O_{14}$, $Mo_{17}O_{47}$ and Mo_4O_{11} were original samples kindly supplied by Dr. L. Kihlborg. $(Ta_{0.07}Mo_{0.93})_5O_{14}$ was prepared as a monophasic sample from appropriate amounts of MoO_3, MoO_2 and Ta_2O_5 by heating at 600 °C for 6 h in a sealed, evacuated silica tube. X-ray diffraction diagrams of the powdered samples did conform to the following published data: $Mo_{18}O_{52}$, ASTM 12-753; $Nb_{0.1}Mo_{0.9}O_{2.80}$ and $Ta_{0.07}Mo_{0.93}O_{2.80}$, Table 2 of ref. [4]; $Mo_{17}O_{47}$, ASTM 13-345; Mo_4O_{11}, ASTM 5-337.

TABLE I. Mixed Valence Molybdenum Oxides, MoO_x.

Compound (x)	Formula	Phase	Structure	Overall Mo oxidation state	Formal Mo(V)/Mo(VI) atomic ratio
2.889	$Mo_{18}O_{52}$	ζ	MoO_3	5.78	0.333
2.800	Mo_5O_{14}	θ	Mixed polygonal	5.60	0.666
2.765	$Mo_{17}O_{47}$	χ	Mixed polygonal	5.53	0.887
2.750	Mo_4O_{11} (m)	η	ReO_3	5.50	1.0
2.750	Mo_4O_{11} (o-rh)	γ	ReO_3	5.50	1.0

Spectroscopic Techniques

XPS spectra of powdered samples were recorded with an AEI ES 200 B spectrometer following the experimental procedure of ref. [3]. IR spectra were obtained on KBr pellet samples using a Beckman 4250 spectrophotometer.

Structural Details

It has been suggested [5] that the facility with which oxygen can be released by MoO_3 may be associated with the formation of crystallographic shear (CS) planes, leading eventually to $Mo_{18}O_{52}$. A further increase in reduction achieving stoichiometry leads to the formation of a new structural device. This is the incorporation of pentagonal columns (PC) as the dominating structural motif of the oxides Mo_5O_{14} and $Mo_{17}O_{47}$. In the two Mo_4O_{11} modifications a somewhat higher degree of reduction is obtained by a structure built up of MoO_4 tetrahedra and MoO_6 octahedra linked by corner-sharing in which PC units are no longer present. In all oxides the molybdenum coordination sphere is invariably complex, covering a wide range of Mo–O distances.

The $Mo_{18}O_{52}$ structure, which may be generalized within the framework of the homologous series Mo_nO_{3n-m+1}, exhibits a marked substructure of the MoO_3-type [6]. The basic layer structure consists of infinite two-dimensional slabs of finite width, which are mutually connected by edge-sharing between component octahedra of neighbouring slabs. The metal coordination of $Mo_{18}O_{52}$ is similar to that of MoO_3 but presents a more pronounced distortion, mainly of the [1 + 1 + 2 + 1 + 1] type. The distortions are greatest close to the shear zone, up to the point that one of the local polyhedra (Mo(17)) is best described as being tetrahedral, leading to a decrease in the number of shared edges (Fig. 1).

Another way for a structure to accommodate moderate reduction is by the introduction of pentagonal columns as in case of Mo_5O_{14}(7) and $Mo_{17}O_{47}$ [8]. In such mixed polygonal networks, which are distinguished by a complicated connection of coordination polyhedra in two dimensions, the equatorial edges of oxomolybdenum pentagonal bipyramids are shared with five octahedra so that there exist pronounced metal atom clusters (Fig. 2). The considerable divergence in Mo–O distances in Mo_5O_{14} can best be described on the basis of one [1 + 2 + 2 + 2] unit and five [1 + 2 + 2 + 1] units. In the latter the prevailing bond distances range from 1.67–1.70 Å, 1.76–1.86 Å, 2.02–2.06 Å and 2.27–2.29 Å.

The oxide Mo_5O_{14}, which exists as a metastable phase [2, 9], is stabilized by partial substitution of Mo by other elements such as V and Nb [10]. Substitution ranges and stabilities of a number of these $(T_x Mo_{1-x})_5O_{14}$ or Θ(T) ternary oxides have been determined [4, 9, 11, 12]. One stable Θ(Nb)-oxide forms

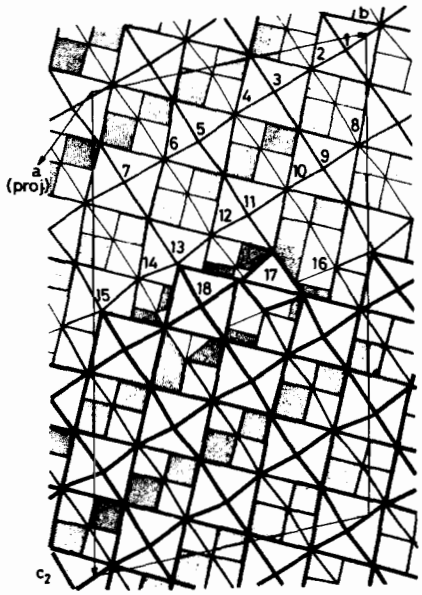

Fig. 1. The structure of $Mo_{18}O_{52}$ visualized as a network of joined MoO_6 octahedra and MoO_4 tetrahedra.

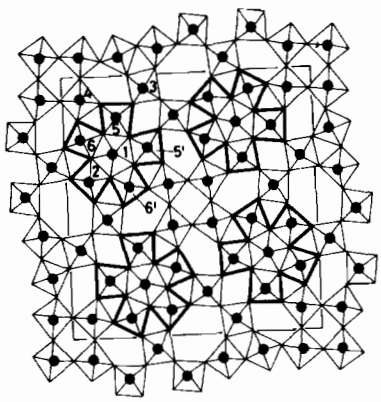

Fig. 2. The crystal structure of Mo_5O_{14}, depicted as a complex of linked pentagonal columns and MoO_6 octahedra, viewed along the short *c* axis.

at $x \simeq 0.09$ in the $Nb_xMo_{1-x}O_{2.80}$ system, which exhibits a narrow composition range [4]. The crystal structure of this compound has not been reported. Ekström *et al.* describe $(V_{0.07}Mo_{0.93})_5O_{14}$ [13], again without structural details. In the corresponding substituted Θ(Ta)-oxide $(Ta_{0.07}Mo_{0.93})_5O_{14}$ tantalum substitutes exclusively in the MO_7 pentagonal bipyramids [14].

The metal atom clusters in the more stable oxide $Mo_{17}O_{47}$ are still further condensed by edgesharing between pairs of octahedra attached to neighbouring pentagonal clusters (Fig. 3). This coupling of PC units involves Mo———Mo bonding (2.639 Å). Considerable variations in Mo–O and Mo———Mo distances accommodate these structural complexities [8]. The asym-

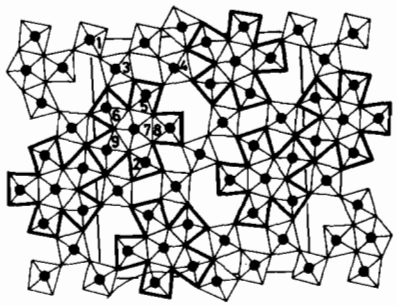

Fig. 3. The crystal structure of $Mo_{17}O_{47}$, depicted as a complex of linked pentagonal columns and MoO_6 octahedra, viewed along the short axis.

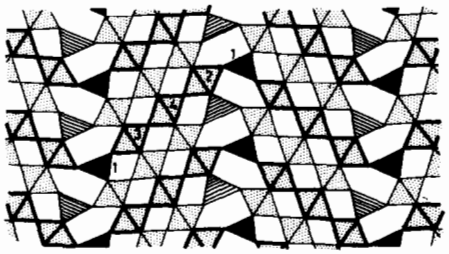

Fig. 4. The crystal structure of orthorhombic Mo_4O_{11}, composed of slabs of ReO_3 type connected by MoO_4 tetrahedra.

metrical unit comprises one pentagonal bipyramid (Mo(7)), three [2 + 2 + 2] oxomolybdenum configurations (Mo(2,4,5)), four [1 + 2 + 2 + 1] distorted molybdenum environments (Mo(1,3,6,8)) and one three-corner displaced arrangement (Mo(9)).

At the lower limit for the formation of oxides containing PC units other structural modes take over such as corner-sharing octahedra and tetrahedra, as in the two Mo_4O_{11} modifications. The two Mo_4O_{11} forms are based on ReO_3, in which slabs of connected octahedra are joined by tetrahedra which share corners with the octahedra of two neighbouring slabs, as shown in Fig. 4 [15]. No tetrahedra or octahedra share edges in these structures. The two Mo_4O_{11} forms differ mainly in the relative orientation of neighbouring slabs. Both modifications show a fairly regular tetrahedral arrangement around one quarter of the metal atoms and a [3 + 3] coordination around the others. This kind of distribution is unique in the molybdenum oxides.

Results and Discussion

Valence Distribution

Table II compares the results of XPS measurements of the reduced molybdenum oxides. Only the high intensity components of the doublets of the 3d and 3p levels are reported as the separation of the components of the doublets was always found to be

TABLE II. Experimental Binding Energies (eV)[a].

Compound	$Mo(3d_{5/2})$	$Mo(3p_{3/2})$
MoO_3	233.5	399.8
$Mo_{18}O_{52}$	233.3 (232.3)	399.5
$(Mo_{0.93}Ta_{0.07})_5O_{14}$	233.3	399.1
$(Mo_{0.90}Nb_{0.10})_5O_{14}$	233.3 (232.4)	399.3
$Mo_{17}O_{47}$	233.3 (232.7)	399.2
Mo_4O_{11}	233.4	399.6

[a]In parenthesis the component at lower intensity.

$E(Mo3d_{3/2}) - E(Mo3d_{5/2}) = 3.0$ eV and $E(Mo3p_{1/2}) - E(Mo3p_{3/2}) = 17.4$ eV for the compounds investigated. Deconvolution of the Mo(3d) levels of $Mo_{18}O_{52}$, M_5O_{14} ($M = Nb_{0.10}Mo_{0.90}$) and $Mo_{17}O_{47}$ indicates two non-equivalent molybdenum atoms. The $Mo3d_{5/2}$ binding energy (233.3 eV) associated with the highest positively charged molybdenum atoms, is practically equal to that observed in MoO_3 (233.5 eV) and may be ascribed to Mo(VI) atoms. The component at lower energy indicates the presence of reduced molybdenum species. If we consider the linear dependency of the Mo(3d) binding energy and the oxidation number, according to Haber *et al.* [16], then the observed ΔE_b (from −0.6 to −1.0 eV) may be interpreted as corresponding to a unitary variation in oxidation number and therefore suggests the presence of Mo(V) atoms.

Deconvolution of the Mo(3d) bands of M_5O_{14} ($M = Ta_{0.07}Mo_{0.93}$) and Mo_4O_{11} is less significant than in the other mixed oxides even though the shape of the photoelectronic signal differs from that in compounds with unmixed Mo valency states. In particular, the minimum between the components of the Mo(3d) doublet is of higher intensity than usual and points to the presence of non-equivalent molybdenum atoms, with one state at lower occupancy than the other. Similar trends in chemical shifts are also observed for energy variations of the Mo(3p) level. The Mo(3p) core level of the polynuclear compounds is less adequate in revealing fine structure due to its inherently higher band width. Therefore, deconvolution of the 3p band and resolution of the two components associated with different molybdenum cations is more difficult.

In the evaluation of the data it is to be taken into account that XPS is a surface technique. The absence of a clear Mo(V) signal for Mo_4O_{11}, which has the maximum calculated value of the formal Mo(V)/Mo(VI) ratio, may be explained if Mo(V) surface sites are greatly oxidized. Differences in Mo(V) distribution in surface and bulk probably also account for

TABLE III. Bond Strength Sums (v.u.) in Mixed-valence Molybdenum Oxides[a].

Atom[b]	$Mo_{18}O_{52}$	Mo_5O_{14}	$Mo_{17}O_{47}$	Mo_4O_{11}(m)	Mo_4O_{11}(o-rh)
Mo(1)	5.39	4.96	5.35	6.06	6.50
Mo(2)	5.62	6.49	5.46	5.99	6.65
Mo(3)	5.86	5.82	5.64	5.67	5.54
Mo(4)	5.90	5.57	5.25	5.02	5.04
Mo(5)	6.13	5.67	5.80	–	–
Mo(6)	5.49	6.60	5.72	–	–
Mo(7)	5.65	–	5.80	–	–
Mo(8)	5.65	–	6.09	–	–
Mo(9)	5.92	–	4.40	–	–
Mo(10)	5.60				
Mo(11)	5.57				
Mo(12)	5.58				
Mo(13)	6.70				
Mo(14)	6.01				
Mo(15)	4.68				
Mo(16)	6.73				
Mo(17)	6.22				
Mo(18)	5.26				
E.s.d.[c]	0.25	0.40	0.60	0.08	0.20
Average	5.78	5.85	5.50	5.68	5.93
Theor.	5.78	5.60	5.53	5.50	5.50

[a]Bond-strength equation: $s = (d/1.882)^{-6.0}$. [b]Cation numbering scheme in accordance with the original papers. [c]σ_s has been calculated for the shortest d_{Mo-O}.

the fact that there is no correspondence between the areas of the Mo(V) and Mo(VI) signals and the calculated Mo(V)/Mo(VI) ratio.

It is known that appearance of two peaks for an inner-shell transition does not prove the existence of a trapped-valence ground state [17]. However, the distribution of the Mo valence population over the available cation sites can be derived from consideration of the Mo–O bond strengths (s) according to the relation $s_{Mo-O} = (d_{Mo-O}/1.882)^{-6.0}$ [1, 18]. Table III shows that the bond strength sums vary considerably between the different coordination polyhedra and (apart from orthorhombic Mo_4O_{11}) give average values fairly close to the formal oxidation number of the compounds. Although calculated bond-strength sums give occasional indications (Mo(15) in $Mo_{18}O_{52}$ and Mo(9) in $Mo_{17}O_{47}$) for a Mo(IV) contribution, this is not corroborated by XPS data, eventually being an effect too weak to be observed. Apparently only in tetrahedral cation sites a Mo(VI) valency is trapped systematically (Mo(17) of $Mo_{18}O_{52}$; Mo(1) of both Mo_4O_{11} polymorphs), as opposed to extensive electron delocalization or a statistical distribution of Mo(V) and Mo(VI) cations at the other molybdenum sites. This is in accordance with the facts that Mo^{6+} ions in tetrahedral sites are extremely stable and that tetrahedral coordinations are practically restricted to hexavalent molybdates, while octahedral coordinations are found for Mo(IV), (V) and (VI).

Structural data are not of high enough accuracy for distinguishing valence states with the same degree of confidence as was possible for $TeMo_5O_{16}$ [3]. However, although the stoichiometry of Mo_4O_{11} is compatible with the existence of one Mo(IV) for every three Mo(VI) atoms or one Mo(V) for every Mo(VI) (corresponding in both cases to a class I mixed valence system in Robin and Day's terminology [19]), it is apparent from Table III that this is not an appropriate description. The calculated bond strengths for both modifications suggest an increase in valence state of the metal atoms from the middle of the basic ReO_3 slabs towards the outside, as already noticed before [20]. At the same time, the distortions within the basic structure decrease from the boundaries of the slabs towards the middle. The average Mo–O distance in the almost regular octahedra around Mo(4), which amounts to 1.94 Å for both Mo_4O_{11} modifications, differs considerably from that expected (1.882 Å) for a regular sixfold oxomolybdenum (VI) coordination [1]. An almost regular sixfold environment has also been found in $Mo(PQ)_3$ (average 1.961 Å, range 1.939–1.988(5) Å) [21], but with a calculated overall valence state as low as 4.70 v.u.

The structure of $Mo_{18}O_{52}$ is rather complex and the interatomic distances are of too low an accuracy to permit a similar interpretation as in case of Mo_4O_{11}. In $Mo_{17}O_{47}$ the e.s.d. values are even higher.

Nevertheless, while the sum of the bond-strengths to Mo(1–8) ranges from 5.2 to 6.1 v.u., the much lower value of 4.40 v.u. is obtained for Mo(9), which is at 2.639 Å distance from the symmetry related atom Mo(9′) by edge-sharing of the polygonal columns. As a low valence is a natural consequence in the presence of a metal–metal bond involving d-electrons, it would appear that the calculated values are more reasonable than the e.s.d. value suggests. Apart from Mo(9), the remaining edge-sharing octahedra around Mo(2,5,6, 8), which form the PC together with the pentagonal MoO_7 bipyramid at Mo(7), have an average bond-strength sum of 5.77 v.u. (range 5.46–6.09 v.u.) with 5.80 v.u. for Mo(7). This is to be compared to an average value of 5.41 v.u. for the Mo(1,3,4) octahedra (range 5.25–5.64 v.u.) joined only through their apices. No obvious relation exists between calculated *s*-values and the distortion of the oxomolybdenum coordination.

A similar trend as found in $Mo_{17}O_{47}$ is observed in Mo_5O_{14} with a mean bond-strength sum of 6.20 v.u. for the MoO_6 units of the PC (Mo(2,5,5′,6,6′)) and 5.70 v.u. for the remaining corner-sharing octahedra centered at Mo(3,4). However, the MoO_7 unit shows a much lower value (4.96 v.u.) than in case of the $Mo_{17}O_{47}$ structure and is closer to that in $(Mo_{0.93}Ta_{0.07})_5O_{14}$ (5.12 and 5.22 v.u. after correction for the Ta-O contribution). Although the valence states in the pentagonal bipyramids of Mo_5O_{14} and $Mo_{17}O_{47}$ are dissimilar, this is not necessarily contradictory, though requires further investigation. Pentagonal bipyramids are also observed in single valence Mo(VI) oxides [22].

The results reported here, namely the presence of metal ions in $Mo_{18}O_{52}$, Mo_5O_{14}, $Mo_{17}O_{47}$ and Mo_4O_{11} in very similar ligand fields, differing from one another by distortions up to a few tenth Å, with some valencies distinguishable but otherwise with considerable delocalization, indicate class II mixed valence systems in Robin and Day's classification [19]. Previously, these oxides have been described as class III B systems [19], as deduced on the basis of the low resistivities of these oxides [2, 23], which seem to indicate that no definite lattice sites are to be allocated to specific valence states in these compounds. The mixed valence transitions in the visible region, which account for the colour of the reduced molybdenum oxides are in accordance with our interpretation. The observed valence distribution may partly be a result of the considerable variations in Mo–O and Mo– – –Mo distances needed to accommodate the geometrical complexities of ordered MoO_x, although of course oxomolybdenum structures are highly distorted even in the absence of mixed valence interaction.

Infrared Spectra

No earlier attempts have been reported on the assignment of Mo–O stretching modes in mixed molybdenum oxides. This is undoubtedly on account of their structural complexity (Tables III, IV) and highly distorted cation environments. Infrared vibration frequencies (Fig. 5) were assigned on the basis of a comparison of experimental data with calculated values taken from the relationship between force constant and bond length [3], as reported in Table V. On the basis of the calculated bond strength distribution and criteria used previously [3] we consider the

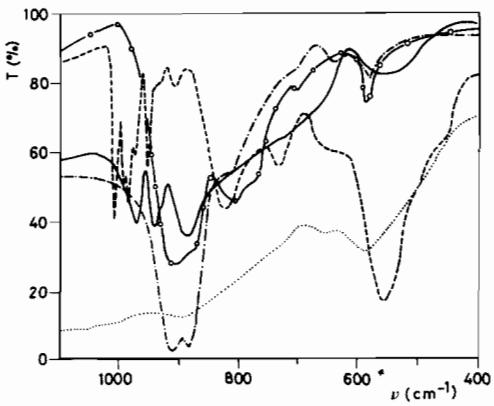

Fig. 5. Infrared spectra in KBr pellets of Mo_4O_{11} (——); $Mo_{18}O_{52}$ (– – – –), $Mo_{17}O_{47}$ (• • • • •), $(Mo_{0.93}Ta_{0.07})_5O_{14}$ (— • — •) and $(Mo_{0.90}Nb_{0.10})_5O_{14}$ (— o —). Mo

TABLE IV. Site Symmetry of Oxomolybdenum Units.

Compound	Factor Group	Z[a]	Site Symmetry	Ref.
$Mo_{18}O_{52}$	$P\bar{1} \equiv C_i^1$	2	C_1	b
Mo_5O_{14}	$P4/mbm \equiv D_{4h}^5$	32	C_1, C_m	c
$Mo_{17}O_{47}$	$Pba2 \equiv C_{2v}^8$	2	C_1, C_2	d
Mo_4O_{11}(m)	$P2_1/a \equiv C_{2h}^5$	4	C_1	e
Mo_4O_{11}(o-rh)	$Pnma \equiv D_{2h}^{16}$	4	C_m	e

[a]Number of molecules per unit cell. [b]Ref. [6]. [c]Ref. [7]. [d]Ref. [8]. [e]Ref. [15].

TABLE V. Infrared ν(Mo–O) Stretching Frequencies (cm^{-1}).

Compound	Mo–O (Å)	B.s. (v.u.)	ν(Mo–O)[a]	C.N.
Mo_4O_{11} (orthorhombic)	1.70–1.90	1.85–1.00	970 (m); 940 (m) 885 (m, br)	3
	2.00	0.7	550 (w, br)	3
M_5O_{14} ($M = Mo_{0.93}Ta_{0.07}$)	1.67–1.70	2.0–1.85	950 (sh)	1
	1.76–1.86	1.50–1.10	905 (s); 875 (s) 825 (sh)	2
	2.02–2.06	0.65–0.60	575 (w)	2
	2.27–2.29	0.30	[b]	1
$Mo_{18}O_{52}$	1.63–1.70	2.4–1.85	1010 (s); 992 (m) 985 (s); 975 (sh) 952 (m)	1
	1.74–1.83	1.60–1.20	830 (s, br)	1
	1.86–1.97	1.10–0.75	730 (m, br); 650 (sh)	2
	2.10–2.20	0.50–0.40	550 (v. s., br)	1
	2.25–2.40	0.34–0.23	[b]	1

[a] w = weak, m = medium, s = strong, v = very, sh = shoulder, br = broad. [b] Unidentified bands in the δ (O–Mo–O) deformation range [24–26].

stretching modes of Mo–O bonds with greatly different bond strengths to be completely independent. We therefore assume that vibrational coupling occurs only for stretching modes of Mo–O bonds of similar bond strength. Mo–O bond lengths and bond strengths have been grouped together in correspondence to IR bands within restricted spectral absorption ranges. Calculated values are not compared to observed ones in Table V as they were only used to establish the expected spectral range for a specific bond strength value. A more detailed examination was not possible in view of the complexity of the oxide structures examined with their impressive variety of bond distances, and lack of Raman spectra, due to the dark appearance of the oxides ($Mo_{18}O_{52}$: bluish black; Mo_5O_{14}: blue violet; $Mo_{17}O_{47}$: reddish blue; Mo_4O_{11}: wine red).

As to the prevalent [3 + 3] oxomolybdenum environment in Mo_4O_{11} (except for the tetrahedral arrangement around Mo(1)), Table V reports separately the three short bonds in the range 1.70–1.90 Å, and the mean value of the three long bonds (2.00 Å). As may be understood on the basis of *s–d* curves, it was not possible to reproduce the spectra using the mean value of the three short bonds as this would otherwise not explain IR bands above 850 cm^{-1}.

M_5O_{14} ($M = Mo_{0.93}Ta_{0.07}$) and $Mo_{18}O_{52}$ have been treated as [1 + 2 + 2 + 1] and [1 + 1 + 2 + 1 + 1] oxomolybdenum coordinations, respectively, with the Mo–O distance ranges as indicated in Table V. The infrared spectrum of M_5O_{14} ($M = Mo_{0.90}Nb_{0.10}$) is similar to that of the analogous compound stabilized by the presence of tantalum (Fig. 5).

The infrared spectrum of $Mo_{17}O_{47}$ is featureless with broad regions of absorption. This may stand in

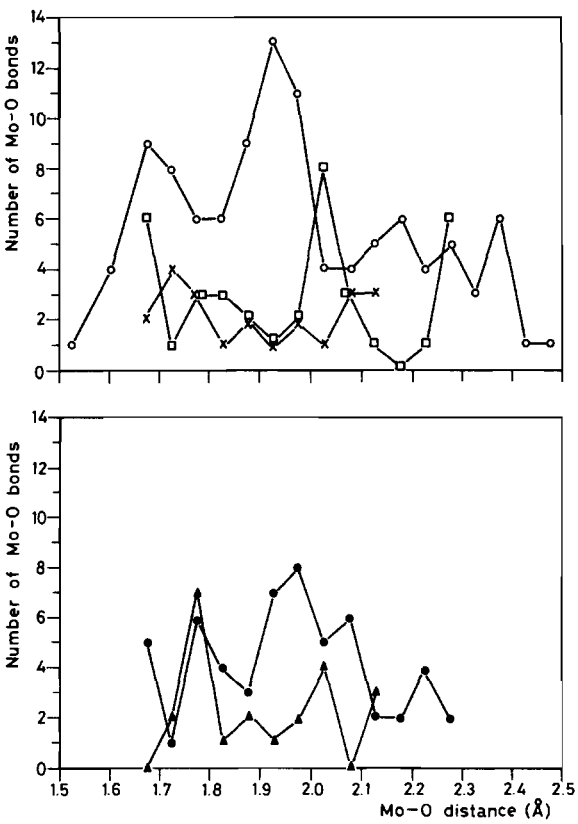

Fig. 6. Histogram of Mo–O distances in oxomolybdenum polyhedra of $Mo_{18}O_{52}$ (○), Mo_5O_{14} (□), $Mo_{17}O_{47}$ (●), monoclinic (▲) and orthorhombic (×) Mo_4O_{11}.

relation to the fact that this oxide contains a wide variety of oxomolybdenum coordinations (see above), as also illustrated by the wide scatter of Mo–O values of Fig. 6. A correlation of infrared data with bond-strengths has therefore not been attempted.

Acknowledgements

Thanks are due to Dr. Lars Kilhborg (University of Stockholm) for providing the original samples.

References

1 J. C. J. Bart and V. Ragaini, *Inorg. Chim. Acta, 36,* 261 (1979).
2 L. Kihlborg, *Acta Chem. Scand., 13,* 954 (1959).
3 J. C. J. Bart, F. Cariati and A. Sgamellotti, *Inorg. Chim. Acta, 36,* 105 (1979).
4 T. Ekström and M. Nygren, *Acta Chem. Scand., 26,* 1836 (1972).
5 F. S. Stone, *J. Solid State Chem., 12,* 271 (1975).
6 L. Kihlborg, *Arkiv Kemi, 21,* 443 (1963).
7 L. Kihlborg, *Arkiv Kemi, 21,* 427 (1963).
8 L. Kihlborg, *Acta Chem. Scand., 14,* 1612 (1960).
9 T. Ekström and M. Nygren, *Acta Chem. Scand., 26,* 1827 (1972).
10 L. Kihlborg, *Acta Chem. Scand., 23,* 1834 (1969).
11 T. Ekström, *Acta Chem. Scand., 26,* 1843 (1972).
12 T. Ekström, *Mater. Res. Bull., 7,* 19 (1972).
13 T. Ekström and R. J. D. Tilley, *J. Solid State Chem., 19,* 125 (1976).
14 N. Yamazoe and L. Kihlborg, *Acta Cryst., B31,* 1666 (1975).
15 L. Kihlborg, *Arkiv Kemi, 21,* 365 (1963).
16 J. Haber, W. Marczewski, J. Stoch and L. Ungier, *Ber. Bunsenges. Physik. Chem., 79,* 970 (1975).
17 N. S. Hush, *Chem. Phys., 10,* 361 (1975).
18 I. D. Brown and K. K. Wu, *Acta Cryst., B32,* 1957 (1976).
19 M. B. Robin and P. Day, *Adv. Inorg. Chem. Radiochem., 10,* 247 (1967).
20 L. Kihlborg, *Arkiv Kemi, 21,* 471 (1963).
21 C. G. Pierpont and R. M. Buchanan, *J. Am. Chem. Soc., 97,* 4912 (1975).
22 J. C. J. Bart and N. Giordano, *Gazz. Chim. Ital., 109,* 73 (1979).
23 O. Glemser and G. Lutz, *Z. anorg. allg. Chem., 263,* 2 (1950).
24 P. Tarte and M. Liegeois-Duyckaerts, *Spectrochim. Acta, 28A,* 2029 (1972).
25 M. Liegeois-Duyckaerts and P. Tarte, *Spectrochim. Acta, 28A,* 2037 (1972).
26 H. Jeziorowski and H. Knozinger, *J. Phys. Chem., 83,* 1166 (1979).